Investigation of the relationship between fluvial topography and factors associated with the occurrence of liquefaction

Masashi Kitazawa
The United Graduate School of Agricultural Sciences Ehime University, Ehime, Japan, m-kitazawa@daiichi-c.co.jp

Tadashi Hara
Kochi University, Kochi, Japan, haratd@kochi-u.ac.jp

Noboru Nakajima
Chiken Co,.Ltd., Kochi, Japan, n-nakajima@chiken.com

ABSTRACT: In April 2016, an epicentral earthquake occurred beneath Kumamoto City in Japan. The earthquake caused widespread liquefaction across the city. In particular, the liquefaction was characterized by its continuous linear occurrence along the natural levees. In Japan, the topography formed by rivers is regarded as an important source of basic information for predicting liquefaction. To clarify differences in liquefaction occurrence characteristics is important to improve the accuracy with which the topographical classification can be used to predict liquefaction.

In this paper we report the results of in-situ testing at selected natural levees where linear liquefaction occurred for the purpose of understanding the characteristics of liquefaction in natural levees. For our in-situ testing we adopted the portable dynamic cone penetration test , which was developed in Japan as a way to evaluate the penetration resistance of soil in a highly portable manner using simple equipment.

Keywords: liquefaction; Kumamoto earthquake; natural levee; portable dynamic cone penetration test

1. Introduction

It is known that the microtopography is intimately related to the characteristics of the surface subsoil [1]. Therefore, in Japan, simple liquefaction prediction methods based on microtopographical classification are often applied[2]. At present, microtopographical classification data for Japan are processed digitally and organized as 250 m mesh data[3]. However, some problems on these methods have been indicated, as in the Kumamoto earthquakes where liquefaction occurred in narrow regions that cannot be sufficiently evaluated using a 250 m mesh, or in cases in which the ground characteristics are insufficiently reflected by the microtopographical classification[4].

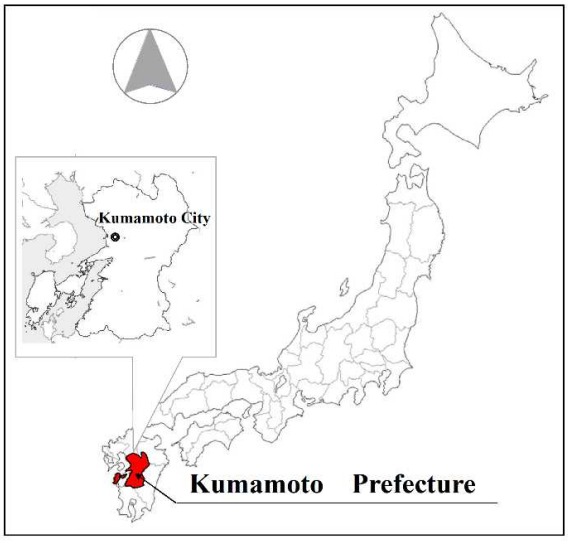

Figure 1. The location of Kumamoto Prefecture in Japan.

In Kumamoto earthquqkes, two earthquakes, the epicenters of which were directly underground, recently occurred near Kumamoto City in Kumamoto Prefecture, which is located in the Kyushu region of southwest Japan(Figure 1), the first one on April 14 and then a second one on April 16, 2016. Severe damage occurred, centering on Kumamoto Prefecture, as a result of the strong tremors during these earthquakes. After these earthquakes, liquefaction occurred over wide areas of ground in Kumamoto City and in adjacent cities and towns, including a natural levee, an old riverbed, and a flood plain, based on their microtopographical classification, and numerous civil engineering and building structures were damaged. In particular, in the southern part of Kumamoto City, in a natural levee where an urban district is situated, limited areas of liquefaction formed, and many residential areas were damaged, including an uneven settlement and an inclined of houses[5].

The natural levee where limited areas of liquefaction occurred during the Kumamoto earthquakes has a fluvial topography formed by river sedimentation, and is a type of microtopography with a high probability of liquefaction [2]. In Japan, which is prone to flood damage, natural levees form slight elevations, and are therefore often used as residential areas safe from flood damage. However, there is a concern regarding the occurrence of disasters owing to their microtopographical classification; therefore, for a natural levee in which a high land use is required, clarifying the relationships among the topography and ground features, as well as the factors that cause liquefaction, regardless of the mesh size, provides important information for improving the precision of liquefaction prediction based on the microtopographical classification.

With the aim of understanding the reasons why differences in liquefaction occur, in this paper, we focus on an area classified as a natural levee. We studied the liquefied

sites of southern Kumamoto City to investigate the differences in the geomaterials between liquefied and non-liquefied sites found in on-site studies. In our research, to understand the penetration resistance of the ground, we used a dynamic cone penetration test (PDCP) developed in Japan, which has high mobility, making it possible to easily understand the penetration resistance of the ground. We also showed that the appropriateness of PDCP is useful for understanding the continuities and minute changes in the ground conditions when the target is sandy soil or fine-grained soil.

The definition of liquefaction used in this paper is based the existence of sand boils and fountains, as obtained from on-site studies and by interviewing local residents. We assumed that the seismic motion, which is the main cause of liquefaction, was the same throughout study region used for the investigation.

2. Overview of Kumamoto earthquake

At 9:26 PM on April 14, 2016, an earthquake (foreshock) with a moment magnitude (Mw) of 6.2 occurred, with its epicenter in Kumamoto Prefecture. Then, at 1:25 AM on April 16, 2016, an earthquake (main shock) of Mw 7.0 occurred with its epicenter in approximately the same location. A intensity of 7 on the Japanese seismic seven-stage scale, the largest value in the Japanese intensity standard, was observed twice in Mashikimachi, which is adjacent to Kumamoto City. This was the first time in Japan that a intensity of 7 on the Japanese seismic scale was observed twice for the same earthquake. The epicenters were near the Hinagu and Futagawa fault zones located in the southeast portion of Kumamoto City, and were inland earthquakes whose epicenters were directly underground [6]. The distribution of the ground acceleration during the main shock is shown in Figure 2 [7]. The peak ground acceleration during the main shock was recorded as 1,326 gal at Mashikimachi, where the amount of damage was high [6].

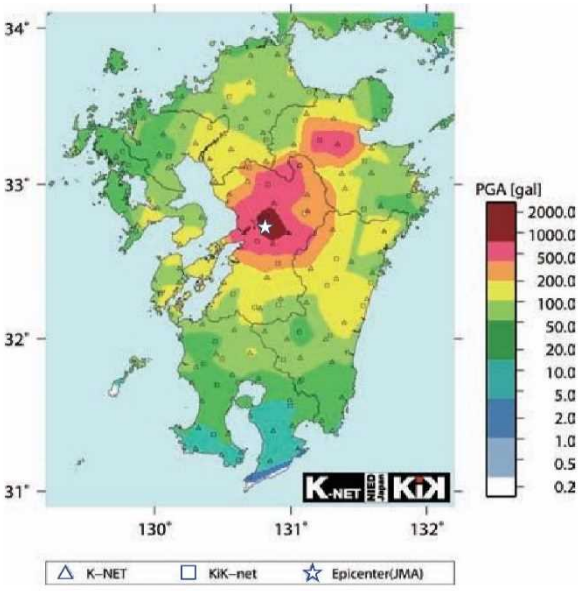

Figure 2. The main-shock earthquake's peak acceleration distribution[7].

3. Investigation area and survey points

3.1. Investigation area

This investigation surveyed the area of southern Kumamoto City, which is indicated by the red border in Figure 3[8], to investigate the factors that caused different liquefaction conditions within the same natural levee. On the northern side of the investigation area is the Shirakawa River, which is the watershed of Mt. Aso, one of the most active volcanoes in Japan. According to a historical document[9], it was estimated that a branch existed in the investigation area 500 years ago, which split from the Shirakawa River. It is thought that each time a flood occurred, gravel flowed from the Shirakawa River into the natural levee, spilling over both banks of the branch, forming a natural levee around it. The natural levee in the invesitgation area corresponds to a part of this. The liquefaction caused by the Kumamoto earthquakes occurred in a band along the current channel, which is part of the old branch. (Figure 3)

3.2. Survey points

We specified a total of four survey points, including both liquefied and non-liquefied points. Maps showing the survey point locations are provided in Figure. 4[10] and 5. To understand the relationship between the ground characteristics and causes of liquefaction, we arranged the survey points at a liquefied area (point A), a non-liquefied area (point C) located away from the channel at approximately 160 m from point A, and at point B where a liquefied area and a non-liquefied area are adjacent within the boundary region where liquefaction occurred.

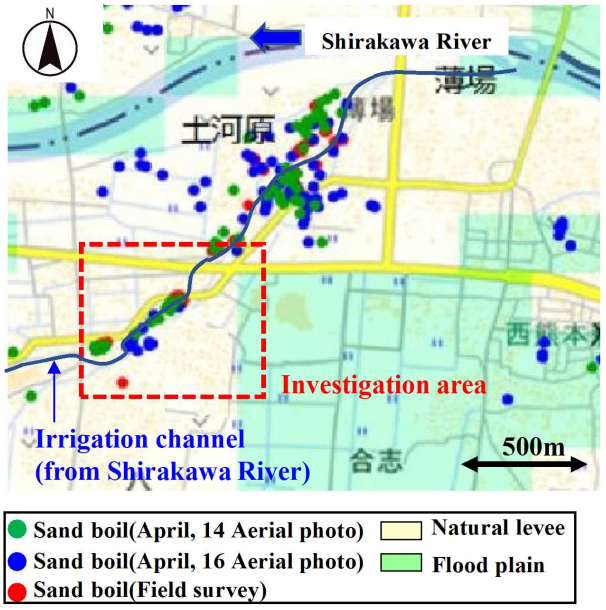

Figure3. The location of investigation area[8].

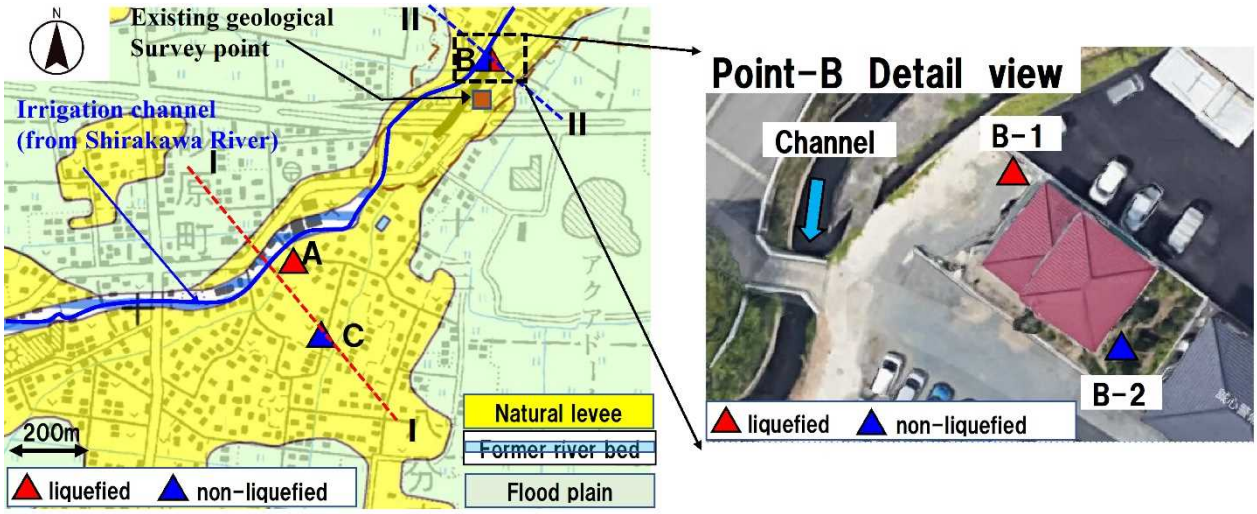

Figure 4. The location of survey points.[10]

Figure 5. The detail view of survey point B.

At point A, sand boils were seen at multiple locations in a plain within a park, and an uneven settlement and inclination were confirmed in nearby houses. Point B was within a residential district, as shown in Figure 5, and two points were specified, namely, a liquefied point B-1 on the side of the channel where liquefaction occurred, and a non-liquefied point B-2 on the other side of the house. At point B-1, near the channel, sand boils and ground cracks were confirmed in multiple locations. Because of the liquefaction, house where the channel side sank by 0.15 m were damaged. Other damage such as from sand boils and ground cracks was unconfirmed in the gardens of private house at point C.

4. Survey method

4.1. Portable dynamic cone penetration test

4.1.1. Test apparatus and equipment

The PDCP test[11] allows a hammer with a mass of 5 ± 0.05 kg to fall freely from a height of 500 ± 10 mm to obtain a dynamic penetration resistance of the ground *in situ*. This test apparatus was an apparatus miniaturized by the Public Works Research Institute of the Ministry of Land, Infrastructure, Transport and Tourism, to survey steep slopes.

This test is widely used to survey the ground surface layer as a simple sounding test and to determine the bearing capacity of small-scale building foundations. The Japanese Geotechnical Society set the standard as JGS-1433 in 1995.[11]

The PDCP apparatus is shown in Figure 6. The status of field survey is shown in Figure 7. The test apparatus consists of a cone, a rod, an anvil, a guidance rod, and a hammer.

4.1.2. Test method and organization of the results

The test procedure was as follows: First, the cone was attached to the tip of the rod, and the anvil, guidance rod, and hammer were attached on top. Next, the test apparatus is maintained in a vertical position above the survey

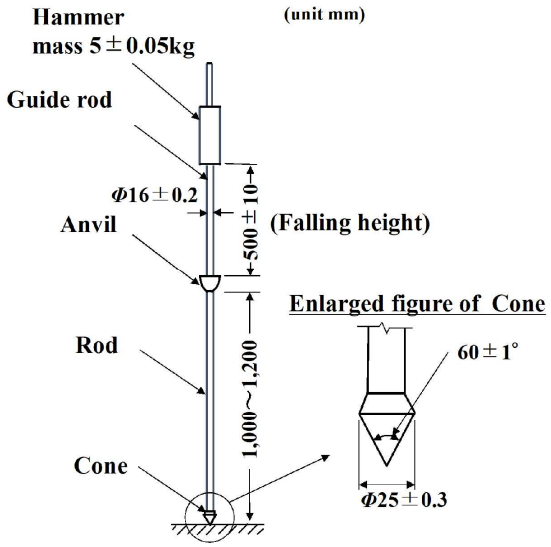

Figure 6. The apparatus of Portable dynamic cone penetration (PDCP).

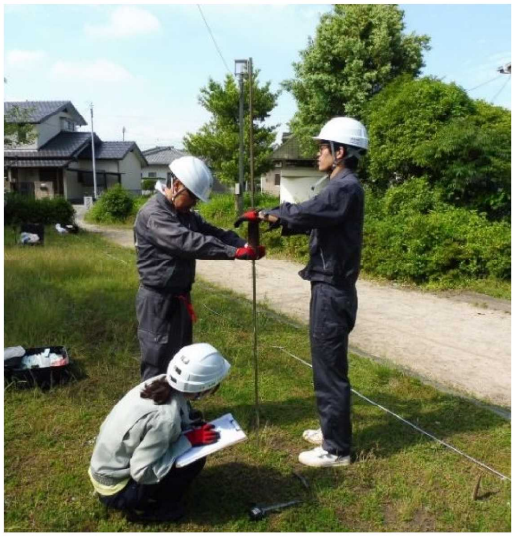

Figure 7. The status of field survey for PDCP.

point allowing the hammer to freely fall. The hammer is dropped freely from a height of 500 ± 10 mm, and the number of blows required to penetrate 100 mm is recorded as the N_d value. If the penetration amount exceeds 100 mm by a blows N_d can be calculated using (1).

$$N_d = 100\frac{N}{\Delta h} \quad (1)$$

where N is the number of blows, and Δh is the penetration amount(mm) .

When the upper part of the rod reaches near the ground surface, the anvil, guidance rod, and hammer are removed for a moment, and the test is continued after adding another rod.

The correlation between N_d value obtained from PDCP and N value obtained from Standard penetration test is shown in (2) and (3). Okada et al. clarified the relationship between N_d value and N value through the results of Swedish sounding test(SWS). In Japan, the following equations are generally applied as a conversion formula for each soil material. [12].

$N_d \leqq 4$

$N = 0.50N_d$ (Gravelly soil)
$N = 0.66N_d$ (Sandy soil)
$N = 0.75N_d$ (Cohesive soil) (2)

$N_d > 4$

$N = 0.7+0.34N_d$ (Gravelly soil)
$N = 1.1+0.30N_d$ (Sandy soil)
$N = 1.7+0.34N_d$ (Cohesive soil) (3)

4.2. Sampling

Because the PDCP cannot confirm the soil properties of the ground, we used a handy geoslicer (HGS)[13] that is able to sample the surface ground with ease. HGS is a method that allows for block sampling (a width of 6 to 10 cm, a depth of up to 3 m, and a thickness of approximately 2 to 3 cm) without disturbing the sediment structure. This allows for a small number of staff members to take samples much more easily compared to the use of a conventional survey apparatus. In the present survey, we used a sample tray that allows for sampling at a maximum of 2.5 m from the ground surface.

4.3. Laboratory soil test

We selected representative samples of the soil layer sampled at each survey point and conducted a density test of the soil particles and a grain size analysis as laboratory soil tests.

5. Survey results

5.1. PDCP results

Figure 8 shows the results of the PDCP at each survey point. The soil was classified based on the HGS sampling result for the surface layer, and based on the PDCP penetration resistance N_d value and existing boring survey results from the surrounding area for the deeper soil.[14]

Point A, a liquefied point, was located 30 m from the channel with nearby liquefaction. The soil property at this point was fine sand from the ground surface to 1.3 m deep. The N_d value of the sand layer within the range of 1.3 m in depth to T.P. 0.5 m, where the N_d value suddenly increases, ranged from 10 to 30 with a mean of 15.7. The groundwater level during the PDCP survey was 1.0 m from the ground surface.

Point B-1 ,a liquefied point, was located 14 m from the channel, and 18 m from point B-2 ,a non-liquefied point. The soil structure was the same for both points, where it was fine sand from the ground surface to 1.0 m. The N_d value for the range of T.P. 3.8 to -0.4 m at point B-1 ranged from 10 to 20 with a mean of 14.0. The N_d values of this range show relatively little variation. At B-2, the

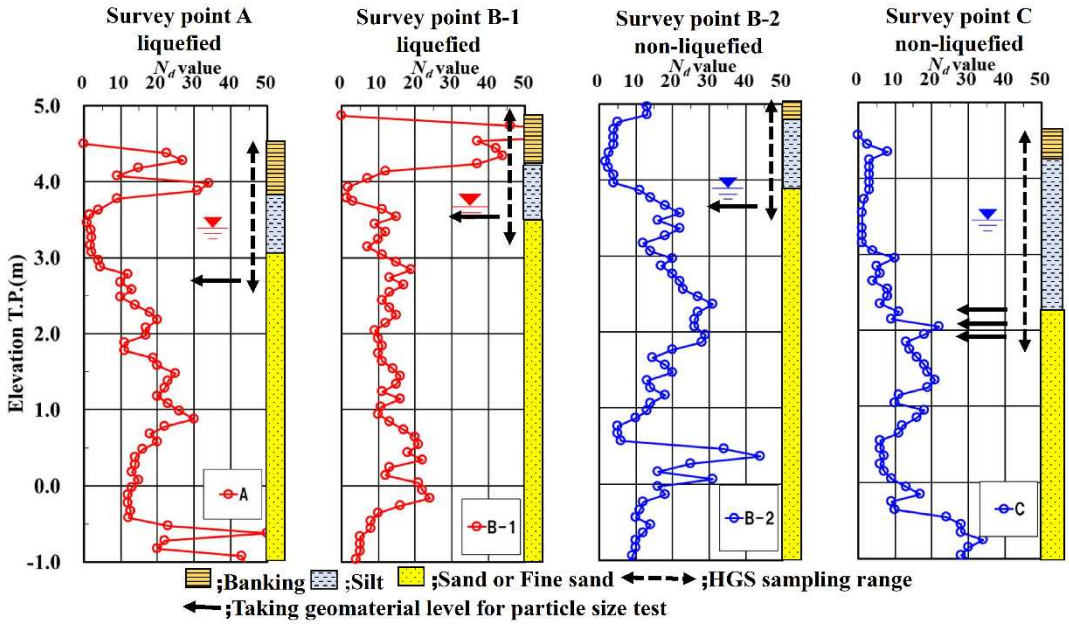

Figures 8. Soil properties assumed based on PDCP and sampling results for the survey points.

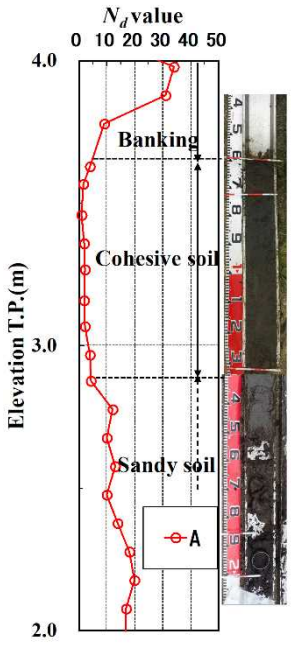

Figure 9. The relationship between $N_d$value and the boundary of soil layer for the sampling geomaterial at point A.

N_d values for the range of T.P. 3.8 to 0.5 m, where the N_d value rapidly increased, ranged from 10 to 30 with a mean of 19.3. Within this range, the penetration resistance was higher than at point B-1.

Point C, a non-liquefied point, was located at approximately 200 m from the channel. The silt layer with an N_d value of less than 10 was thicker than that at other survey points, distributed within a range of up to 2 m from the ground surface. The N_d values within the range of T.P. 3.0 m to -0.25 m ranged from 5 to 20 with a mean of 11.4, which was the lowest N_d value among the survey points. The groundwater level during the survey was the same as that in the other survey points at 1 m from the ground surface.

Within the ranges sampled at each survey point, the position at which the N_d values of the PDCP changed, and the boundary between soil types was consistent. Figure 9 shows the relationship between N_d values and the boundary of soil layer for sampling at point A.

5.2. Particle size composition

At each survey point, we selected representative samples from the sampled range, and conducted a density test of the soil particles and a grain size analysis. Figure 10 shows the particle size composition of samples from each survey point, and Table 1 shows the results of the laboratory soil test.

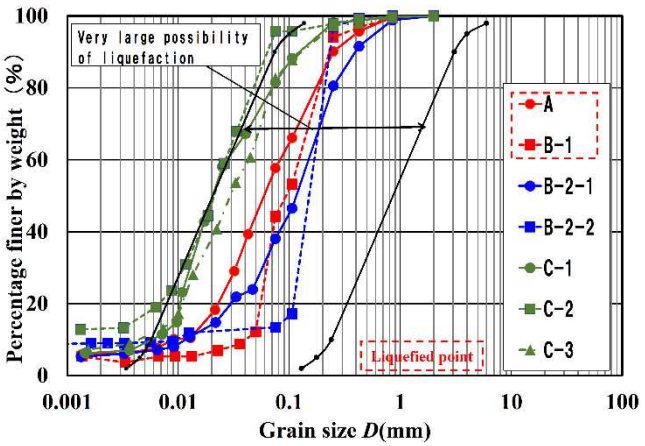

Figure 10. The particle size composition of samples from each survey point.

The Technical Standard and Commentaries for Port and Harbour Facilities in Japan by the Ports & Harbour Association of Japan [15], which is the design standard for ports and harbors in Japan, stipulates the range of grain size with potential for liquefaction based on the existing survey results of liquefaction. We showed that this grain size range has potential for liquefaction as based on the Technical Standard for Port and Harbour (range A) within the particle size composition, and compared the range with potential for liquefaction with particle sizes of the present samples. Points A, B-1, and B-2 have the same fine sands from the ground surface to a depth of 1.5 to 2.0 m. Their particle size composition shows some variations in the fine fraction content (F_c), although the average particle size (D_{50}) and uniformity coefficient (U_c) were similar. The particle size composition of these three points is near the center of range A. The soil layer from the ground surface to a depth of 2.5 m at point C, a non-liquefied point, was silt with F_c of 80% or higher, and its particle size composition was near the smaller limit of range A.

5.3. Other survey findings for reference

At house that were damaged by liquefaction at point B, soil improvement work is being performed to repair the damage caused by land subsidence. During this work, Sweden weight sounding test(SWS), which is often used for residential foundation, is the method used for the ground survey. Currently, owners of this house provided the soil survey results; hence, we compared them with PDCP results to discuss PDCP characteristics. Figure 11 shows the results of SWS near point B-2.

Table 1. The result of laboratory soil test. (Yellow:liquefied point)

Survey Point		Lique-faction occurred	Grand level	Grand water level	Depth of geomaterials		ρ_s	D_{50}	F_c	C_c	I_p	U_c	N_d value	Distance from channel
			(T.P.m)	(T.P.m)	(G.L.-m)	(T.P.m)	(g/cm3)	(mm)	(%)	(%)				L(m)
A	—	Yes	4.50	3.50	-2.00	2.50	2.780	0.061	57.7	6.9	N_p	9.3	10.0	31
B	B-1	Yes	4.87	3.94	-1.50	3.37	2.801	0.095	44.3	4.5	N_p	3.2	12.0	16
	B-2-1	No	5.50	3.80	-2.10	3.40	2.472	0.121	38.1	6.7	—	13.9	19.0	34
	B-2-2	No			-2.20	3.30	2.603	0.165	13.4	9.2	—	19.1	20.0	
C	C-1	No	4.57	3.47	-2.50	2.07	2.696	0.021	81.6	8.7	N_p	4.7	16.0	198
	C-2	No			-2.60	1.97	2.538	0.021	95.8	16.7	—	20.3	20.0	
	C-3	No			-2.70	1.87	2.529	0.030	82.7	10.4	—	9.4	16.0	

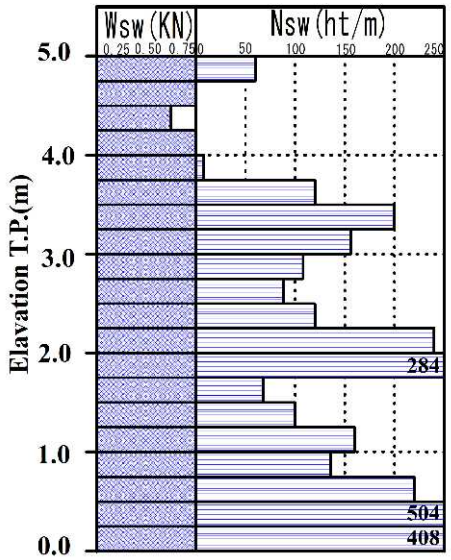

Figure 11. SWS result near point B-2.

6. Discussion

6.1. The relationship between topographic characteristics and liquefied / non-liquefied in natural levees.

Figure 12 shows the cross sections of the survey points A, B, and C that run perpendicular to the flow direction of the channel shown in Figure 4. This Figure shows that natural levees in the surveyed area have a convex shape with peaks near the channel. The Figure also shows a horizontal positional relationship between the channel and each survey point. Liquefied points A and B-1 were located within 40 m of the channel, and at relatively high elevations near the top of the natural levees. The non-liquefied point C was approximately 200 m from the channel, and on the margin of the convex shape at about 1 m below the peak of the cross section. Liquefied points in natural levees within the surveyed area were relatively high points on natural levees, near the current channel. According to a historical document [9], this area was the location of a branch of the main channel of the Shirakawa River, which is the origin of the current channel.

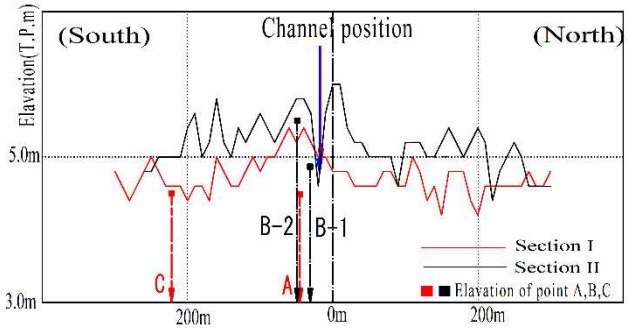

Figure 12. Cross sections at points A and C, B-1 and B-2. (the aspect ratio: 100:1).

6.2. The Relationship between ground characteristics and liquefaction factors in liquefied and non-liquefied points.

We compared ground characteristics of liquefied points and non-liquefied points using PDCP results and the particle size composition at each survey point.

First, we compared PDCP results in the range of T.P. 4.0 to −1.0 m excluding the ground surface for liquefied points, A and B-1 (Figure 13).

At point A, the N_d value ranged from 10 to 30 in the range of T.P. 3.0 to −0.5 m, while the N_d value ranged from 10 to 20 in the range of T.P.3.5 to −0.5 m at point B-1. The geomaterial was fine sands based on the particle size composition. Based on the depth from the ground surface and stratigraphic composition, fine sands in this area are assumed to be the liquefaction layer. We assumed a T.P. value of between 3.0 and 0.0 m from this range to be the liquefaction layer, and showed the N_d (B)/ N_d (A): the ratio of N_d at each depth (Figure 14). In this range, the mean N_d ratio was 1.0. The mean penetration resistance of the ground at both points in the range (assumed to be the liquefaction layer) was equivalent, and the ground characteristic at the liquefied points was considered as fine sands with an N_d value of 10 to 20 (30 in some areas).

At B-1 and B-2 in point B, which is the boundary of the liquefaction occurrence range, we compared PDCP results in the range of T.P. 4.0 to −1.0 m excluding the ground surface (Figure 15). The N_d value at point B-2, which is a non-liquefied point, exceeded the N_d value of liquefied points in the range of T.P. 3.0 to 1.5 m. We present the N_d ratio (N_d (B-2)/ N_d (B-1)) in the range of T.P. 3.0 to 0.0 m, which is assumed to be the liquefaction layer for Point B-1 (Figure 16). Near T.P. equal to 2.0 m, the N_d value for the non-liquefied point was three times that of the liquefied point, where the mean in the selected range is 1.53 times higher. As for the particle size composition at this point, fine sands had slightly larger grain size at point B-2 compared to point B-1. The difference in occurrence of liquefaction at the boundary of the liquefied points was caused by differences in the density of the same fine sands.

Figure 17 shows the comparison of the PDCP results at Point C, which is at a distance from point A, a liquefied point. When compared in the range of T.P. 3.0 to 0.0 m, the N_d value of point A was 20% higher overall. The particle size composition at point C was silt with N_d values of 10 to 20 and F_c of 80% or higher around T.P. equal to 2.0 m. At point C, the N_d value from the survey result alone cannot provide an estimate for fine sand and silt as geomaterials, making particle size composition information necessary. Silt at point C shows a N_d value close to fine sands; thus, this is considered a firm fine-grained soil. The reason for the lack of liquefaction in the areas far from the channel was that the geomaterial is firm fine-grained soil.

Liquefaction occurrence factors in natural levees within the surveyed area are as follows: 1) Liquefied points within a distance of 40 m from the channel were located in high points on the natural levees, and consist of fine sands with an N_d value of 10 to 20. 2) At the

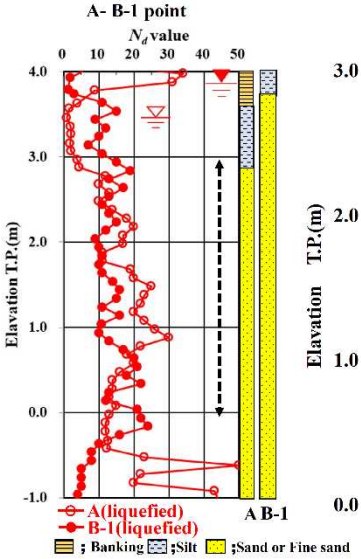

Figure 13. PDCP results at liquefied points A and B-1.

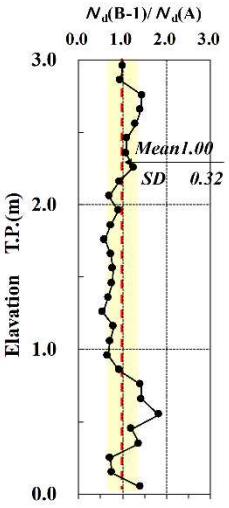

Figure 14. N_d ratio in the range 3.0～0.0m.

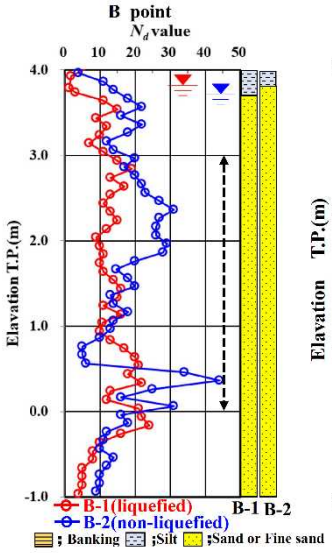

Figure 15. PDCP results at points B-1 and B-2.

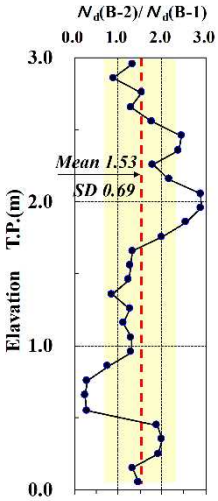

Figure 16. N_d ratio in the range 3.0～0.0m.

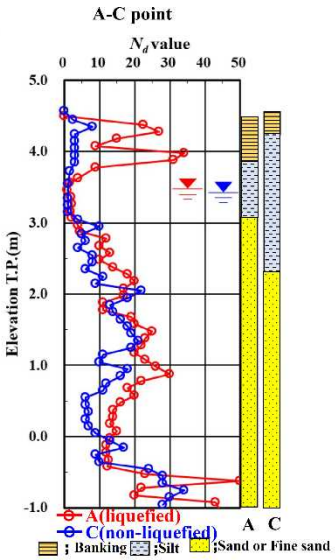

Figure 17. PDCP results at points A and C.

boundary of the liquefied points, occurrence of liquefaction depended on the difference in density caused by different N_d values in the same fine sands. 3) Locations away from the channel, where liquefaction did not occur, were on lower points of the convex natural levees, and consisted of firm silt with a N_d value slightly lower than that of fine sands. Natural levees in the survey area exhibited a trend where ground became finer with the horizontal distance perpendicular to the channel.

6.3. Comparison of PDCP and SWS test results.

Point B-2 was selected for comparison. SWS was performed near this site, and it was one of the B points at which residences sustained liquefaction damage. To compare the PDCP results with the SWS results shown in Figure 11, the experimental data from both penetration tests were converted to *N* value and the results are shown in Figure 18. Equations (2)–(3) and (4) were used to convert the PDCP and SWS results to *N* value, the latter pair had previously been proposed by Inada.[16]

$$\left.\begin{array}{ll} N=2\cdot Wsw+0.067\cdot Nsw & \text{(Sandy soil)} \\ N=3\cdot Wsw+0.050\cdot Nsw & \text{(Cohesive soil)} \end{array}\right\} \quad (4)$$

where W_{SW} is the load applied to penetrate the ground (less than 1kN), and N_{SW} is the number of half-rotations per meter of penetration when the probe was rotated after the penetration of the above load was finished (half-rotations/m).

The ground penetration resistance characteristics were mostly the same, but SWS results for sandy soil tended to be higher than the PDCP results. Depending on the depth of the sand soil, there was a difference of up to two times. N values of 3–14 were observed for fine sand in the range of T.P. 4.0–0.0 m for data from a existing geological survey performed in the vicinity of the survey site[14] (locations shown in Fig. 4; *N* value shown in Fig. 18). Therefore, the PDCP results were closer to the surrounding ground characteristics than the SWS method was, which is a static penetration survey method used for

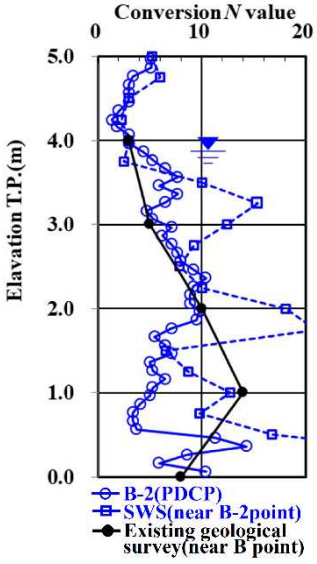

Figure 18. The comparison of PDCP results and SWS results at near point B-2.

load and rotation. Basic penetration was 0.1 m for PDCP, which was denser than the value of 0.25 m for SWS. This shows the continuity of the soil layer in more detail. Sandy soil and fine-grained soil with an N_d of less than 30, which consists of the ground in the case of the natural levees in the survey area, had a PDCP hammering energy less than that of the standard penetration test, which allows for the detection of minor changes in the ground. As shown in Figure 9, the point of change in N_d values was consistent with the soil layer boundary. Depending on the ground, PDCP was simple and the portability was high; thus, if there were any restrictions in time, place, and budget, it could be a useful penetration resistance test.

7. Conclusion

In this study, we identified factors responsible for different manifestations of liquefaction in the same natural levees by performing PDCP and taking samples of materials at liquefied and non-liquefied points to determine their physical properties. Our approach demonstrates the usefulness of simple *in situ* field testing to estimate liquefaction factors in microtopography by determining ground characteristics associated with (1) topological and geological changes that cannot be determined by microtopographic segmentation of digital data, and (2) location in relation to channel, which seemed to promote liquefaction within the scope of this survey. We showed that the PDCP used in the present survey is useful for understanding the continuities and minute changes in the ground conditions when the target is sandy soil or fine-grained soil with an N_d of 30 or less. A mobile, rapid, and flexible survey method in response to topographic characteristics, such as the PDCP method used in the present survey and geomaterial sampling, though simple methods, they are suitable survey methods for determining liquefaction factors in the future.

Acknowledgement

The field survey in the area around the town of Sunahara in Minami Ward, Kumamoto City, the *in-situ* test, and the laboratory test were conducted with the support of Mr. Ryu Shibahara, Mr. Shinjiro Hayashi of Kochi University Geotechnical Engineering Lab and Miss Yurika Nakayama(graduate). We also would like to thank local residents who provided support to the field surveys around the town of Sunahara, along with opening up their properties for *in-situ* tests and surveys that provided valuable soil survey results.

References

[1] Masahiko,O., “Technique and Development of Geomorphologioc Land Classification”, Kokin Shoin, Tokyo,Japan. pp. 2-4,1983.

[2] National Land Agency Disaster Bureau, “Manual for Regional Zooning on Liquefaction (1999 Version)”, National Land Agency Disaster Bureau, Tokyo, Japan, pp44-55. 1999.

[3] Matsuoka, M.,Wakamatsu, K., and Hashimoto, M., ”Liquefaction Potential Estimation Based on the 7.5-arc-second Jpan Engineering Geomorphologic Classification Map”, *Journal of Japan Association for Eartquake Engineering*, Vol.11, No.2, pp. 20-39, 2011. https://doi.org/10.5610/jaee.11.2_20

[4] Yasuda, S., Ishida, E., and Hosokawa, N., “Present and future hazard maps for soil liquefaction”, *Journal of JSCE*, A1, Vol.65, No.1, pp. 188-194, 2009. https://doi.org/10.2208/jscejseee.65.188

[5] Japan Society of Civil Engineers. “Liquefaction dameges”, Report on the Damege Surveys and Investigations Following the 2016 Kumamoto Eathquake, Japan Society of Civil Engineers., Tokyo, Japan, pp. 124-151, 2017.

[6] Japan Meteorological Aency, “The report of Kumamoto earthquake” ,https://www.jma.go.jp/jma/menu/h28_kummoto_jishin_menu.html. [Accessed:15 August 2019]

[7] National Research Institute for Earth Science and Disaster Resilience.K-net,Kik-net, http://www.kyoshin.bosai.go.jp/kyoshin/topics/Kumamoto_20160414/inversion/. [Accessed:28 August 2019]

[8] Wakamatsu, K., Senna, S., and Ozawa, K., “Liquefaction and its Characteristics during the 2016 Kumamoto Earthquake”, *Journal of Japan Association for Eartquake Engineering*, Vol.17, No.4, pp. 81-100, 2017. https://doi.org/10.5610/jaee.17.4_81

[9] The Editional Committee of “New Kumamoto City History”, “The eary modern period Ⅱ”, New Kumamoto City History, Vol.4, Kumamoto City, Kumamoto, Japan, pp. 485-495, 2003.

[10] Geographical Survey Institute, Landform classification map for flood control, https://maps.gsi.go.jp/ [Acessed: 15 August 2019]

[11] Japanese Geotechnical Society, “6. Sounding”, Japanese Standard and Explanations of Geotechnical and Geoenvironmental Investigation Method, Japanese Geotechnical Society, Tokyo, pp. 317-323, 2013.

[12] Okada,T., Sugiyama,T., Muraishi,H., Noguchi,T., “A correlation of Soil Strength between Different Sounding Tests on Embankment Surface”, *Soil and foundation*, Japanese Geotechnical Society, Vol.40, No.411, pp. 11-16, 1992.

[13] Kinoshita,H.,Fujimoto,K., “A study on paleo-sedimentary environment using handy geoslicer in alluvial plain” , Proceedings of 2018 Annual Conference, Japanese Geotechnical Society Shikoku branch, pp. 59-60, 2018.

[14] Japanese Geotechnical Society Kyushu branch, ”The Shared database in Kumamoto prefecture”, The Shared database on Kyushu Geotechnial Information”(CD-ROM), Japanese Geotechnical Society Kyushu branch, Fukuoka, Japan, 2012.

[15] The overseas coastal area development institute of Japan, “Ground Liquefaction”, Technical Standard and Commentaries for Port and Harbour Facilities in Japan. The ports & Harbour Association of Japan, Tokyo, Japan, pp. 282-287, 2012.

[16] Inada, B., “Study on the application of the Swedish Weight Sounding test”, *Soil and foundation*, Japanese Geotechnical Society, Vol.8, No.1, pp.13-18, 1960.